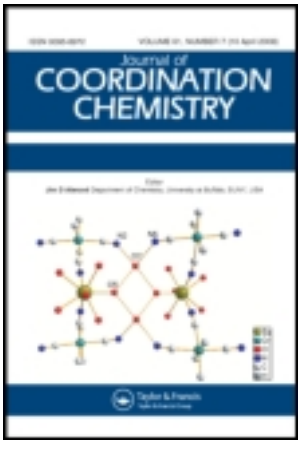

Journal of Coordination Chemistry
Publication details, including instructions for authors and subscription information:
http://www.tandfonline.com/loi/gcoo20

Two dinuclear Schiff-base complexes: synthesis, characterization, and biological activity

Yun-Feng Chen [a], Lai Wei [a], Jun-Lin Bai [a], Hong Zhou [a], Qi-Mao Huang [a], Jun-Bo Li [a] & Zhi-Quan Pan [a]

[a] Key Laboratory for Green Chemical Process of Ministry of Education, Wuhan Institute of Technology, Wuhan 430073, P.R. China

Published online: 04 Apr 2011.

To cite this article: Yun-Feng Chen, Lai Wei, Jun-Lin Bai, Hong Zhou, Qi-Mao Huang, Jun-Bo Li & Zhi-Quan Pan (2011) Two dinuclear Schiff-base complexes: synthesis, characterization, and biological activity, Journal of Coordination Chemistry, 64:7, 1153-1164

To link to this article: http://dx.doi.org/10.1080/00958972.2011.563846

Journal of Coordination Chemistry
Vol. 64, No. 7, 10 April 2011, 1153–1164

Two dinuclear Schiff-base complexes: synthesis, characterization, and biological activity

YUN-FENG CHEN, LAI WEI, JUN-LIN BAI, HONG ZHOU, QI-MAO HUANG, JUN-BO LI and ZHI-QUAN PAN*

Key Laboratory for Green Chemical Process of Ministry of Education, Wuhan Institute of Technology, Wuhan 430073, P.R. China

(*Received 19 October 2010; in final form 10 January 2011*)

Two complexes, $[Zn_2L(\mu\text{-}OAc)](ClO_4)$ (**1**) and $[Mn_2L(OAc)_2]\cdot 4H_2O$ (**2**), were synthesized by [2 + 2] cyclo-condensation between 2,6-diformyl-4-fluorophenol and 1,3-propyldiamine in the presence of metal ions M(II) (M = Zn and Mn), and were characterized by chemical analyses, IR spectra, electrospray mass spectra, and X-ray determinations. The results show that **1** forms dimers through hydrogen bonding. In **2**, lattice waters, forming a 1-D water chain, function as glue to form a 3-D supramolecular network through extended hydrogen bonding. *pBR322* plasmid DNA can be transformed to nicked form in air by **1** or nicked and linear forms in air by **2**. Moreover, their antibacterial activities against *S. aureus* were investigated using penicillin as reference system.

Keywords: Cyclo-condensation reaction; Macrocyclic compound; DNA cleavage; Antibacterial activities

1. Introduction

Macrocyclic ligands and their complexes have been extensively studied [1]. Dramatic progress has been achieved in macrocyclic chemistry with various applications in catalysis and biology [2]. At the same time, Schiff bases have drawn much attention because of their potential application in medicine; many show anti-inflammatory activity [3]. There are also some examples with antibacterial, antifungal, and anticancer activities [4], and some have been used to design medicinal compounds [5]. As a result, considerable interest is centered on investigation of the relationship between the structures and biological activities of Schiff-base metal complexes [6].

Also, study on various water assemblies in different crystalline materials has become a popular research field in attempts to provide insight into the properties of bulk water in its liquid and biological systems. The assembly modes vary as separated or bonded water clusters. Some extend through hydrogen-bonding interactions into 1-D, 2-D, or 3-D networks. Although there are a few examples where single molecules are

*Corresponding author. Email: zhiqpan@163.com

Journal of Coordination Chemistry
ISSN 0095-8972 print/ISSN 1029-0389 online
DOI: 10.1080/00958972.2011.563846

interconnected by 1-D water chains, none of them have a macrocyclic complex and two kinds of water chains alternating.

Our group showed that Schiff-base metal complexes derived from salicylaldehyde have better biological activities [7, 8]. Within our ongoing studies on the biological activity of various transition metal complexes, herein, two new Schiff-base metal (Zn^{2+}, Mn^{2+}) complexes were synthesized and their antibacterial activities were investigated. The macrocyclic ligand is shown in scheme 1. The crystal structure of the dinuclear Mn(II) macrocyclic complex shows that there are two kinds of water chains in the complex. To the best of our knowledge, this is the first example of water chains in a macrocyclic complex.

2. Experimental

2.1. *Materials and preparation*

All solvents and chemicals were of analytical grade and used as received, except methanol that was purified to absolute by the general method. 2,6-Diformyl-4-fluorophenol

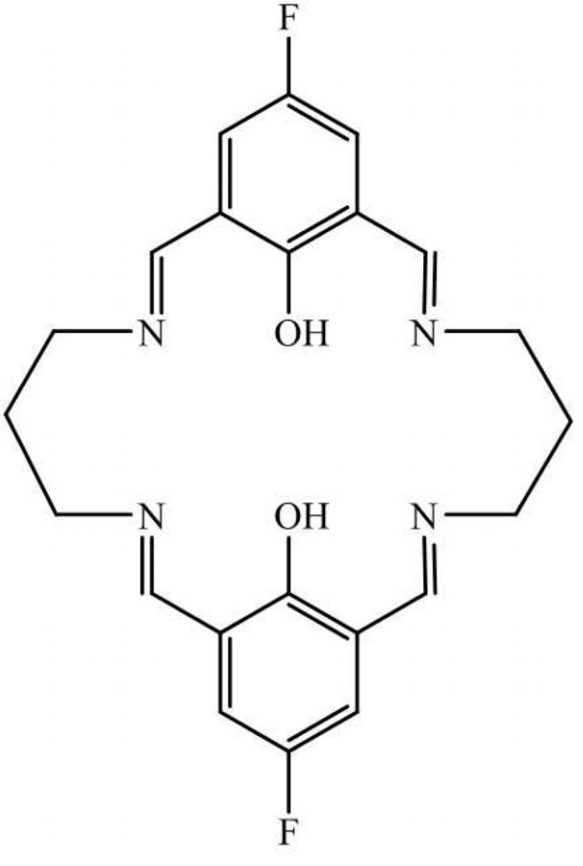

Scheme 1. The molecular structure of H_2L.

was prepared according to literature methods [9]. Tetrabutylammonium perchlorate was recrystallized biquadratically before use. Tris(hydroxymethyl)amino-methane (Tris), bromophenol blue, ethidium bromide (EB), agarose gel, and plasmid *pBR322* DNA were purchased from TOYOBO Co. *Escherichia coli* and *Staphylococcus aureus* were obtained from Huazhong University of Science and Technology.

Buffer solutions were prepared with doubly distilled water. TAE buffer: 121 g Tris-HCl, 28.5 mL acetic acid, and 18.6 g EDTA in 500 mL water, pH = 8; reaction solution: 121 g Tris-HCl, 28.5 mL acetic acid, and tetrabutylamine perchlorate in 500 mL DMF–water solution; BSE solution: 0.25% bromophenol blue, 40% (W/V) saccharose, 10% (W/V) EDTA, and keeping at 4°C; EB solution: EB 0.1 g in 100 mL water.

2.2. *Physical measurement*

IR spectra were measured using KBr disks on a Vector 22 FI-IR spectrophotometer. Electrospray mass spectra (ES-MS) were determined on a Finnigan LCQ ES-MS mass spectrograph using methanol as the mobile phase with a sample concentration of about 1.0 mmol dm^{-3}. The diluted solution was electrosprayed at a flow rate of 5×10^{-6} dm^3 min^{-1} with a needle voltage of +4.5 kV. The temperature of the heated capillary in the interface was 200°C and a fuse silica sprayer was used.

2.3. *Crystal structure determination*

Diffraction intensity data were collected on a SMART-CCD area-detector diffractometer at 293 K using graphite-monochromated Mo-Kα radiation ($\lambda = 0.71073$ Å). Data reduction and cell refinement were performed by SMART and SAINT Programs [10]. The structure was solved by direct methods (Bruker SHELXTL) and refined on F^2 by full-matrix least squares (Bruker SHELXTL) using all unique data [11]. The non-H atoms in the structure were treated as anisotropic. Hydrogens were located geometrically and refined in riding mode.

2.4. *Preparation of the complexes*

$[Zn_2L(\mu\text{-OAc})](ClO_4)$ (**1**): To a refluxing solution of 2,6-diformyl-4-fluorophenol (0.101 g, 0.60 mmol) in absolute methanol (15 mL) was added a solution of hydrated zinc acetate (0.067 g, 0.30 mmol). The solution was stirred vigorously while a methanolic solution (10 mL) of 1,3-diaminopropane (0.46 mmol, 0.60 g) was added slowly. After addition was complete, the resulting solution became orange, and then triethylamine (*ca* 1 mL) was added, followed by refluxing for 6 h. The hydrated zinc perchlorate (0.093 g, 0.42 mmol) was added to this solution, and the solution was stirred for 4 h and ether (50 mL) was added to precipitate the product. The powder precipitated was filtered off, washed with ether, and dried in air (yield 0.496 g, 70.9%). Orange block crystals suitable for X-ray diffraction were obtained by evaporating the methanol solution of the complex. Anal.: Found (%): Zn, 18.70; F, 5.40. Calcd (%) for $C_{24}H_{23}ClF_2N_4O_8Zn_2$: Zn, 18.79; F, 5.43. IR (KBr, ν/cm^{-1}): 1644 ($\nu_{C=N}$), 1076, 624 (ν_{ClO4}). UV (DMF, λ_{max}, nm): 283, 378 (s).

$[Mn_2L(OAc)_2]\cdot 4H_2O$ (**2**): **2** was prepared by a similar procedure as described above, except that $Mn(OAc)_2{\cdot}2H_2O$ and $Mn(ClO_4)_2{\cdot}6H_2O$ were used instead of $Zn(OAc)_2\cdot 2H_2O$ and $Zn(ClO_4)_2{\cdot}6H_2O$, respectively. Yield: 0.568 g, 80%. Anal.: Found (%): Mn, 15.40; F: 5.32. Calcd (%) for $C_{26}H_{34}N_4F_2Mn_2O_{10}$: Mn, 15. 47; F, 5.35. IR (KBr, ν/cm^{-1}): 3400 (ν_{OH}), 1649 (C=N), 1121 (ν_{ClO4}), and 620 ($\delta_{ClO_4^-}$).

2.5. *DNA cleavage*

DNA cleavage reactions were carried out in a total volume of 1 μL containing 0.25 μg plasmid *pBR322* DNA in the presence of an appropriate amount of the complexes. Agarose slab gels were prepared by adding agarose (0.5 g) to a hot TAE solution (50 mL) before cooling to room temperature. The complexes (0.5 μL) and DNA (0.5 μL) were placed in the bottom of the gels in a reaction solution (1.5 μL). After incubation for 3 h in a covered heating block, the reactions were quenched by the addition of BSE solution. One microliter samples were electrophoresed for 3 h at 120 V on agarose slab gels. The gels were then stained using EB solution and photographed on VL E-BOX Gel Imaging System. All the experiments were performed at room temperature unless otherwise noted.

2.6. *Antibacterial activity*

The synthesized compounds were tested for their *in vitro* antibacterial activity against Gram-positive (*S. aureus*) and Gram-negative (*E. coli*) bacteria using the paper disk diffusion method [4] for qualitative determination. The bacterial strains were cultured on nutrient medium and the broth media were incubated for 24 h.

For preparation of disks and inoculation, 1.0 mL of inoculates were added to 50 mL of agar media (40–50°C) and mixed. The agar was poured into 120 mm petri dishes and allowed to cool to room temperature. Wells (6 mm diameter) were cut in the agar plates using proper sterile tubes and the wells were filled with a solution of 0.1 mL of the complexes dissolved in DMSO. The plates were left on a level surface, incubated for 24 h at 37°C for the bacteria and then the diameter of the inhibition zones was read. The inhibition zone formed by these compounds against the particular test bacterial strain determined the antibacterial activities of the compounds. The mean value obtained for three individual replicates was used to calculate the zone of growth inhibition of each sample. Both antimicrobial activities were calculated as a mean of three replicates.

3. Results and discussions

3.1. *Synthesis and characterization*

Owing to the existence of fluorine in the complexes, the C, H, and N contents cannot be detected by elemental analyzer. The contents of metals and fluorine were determined by general chemical methods. The acquired results are in agreement with the compositions of the complexes. In IR spectra of the complexes, the strong band of the carboxyl absorption at 1694 cm^{-1} in 2,6-diformyl-4-fluorophenol disappeared and sharp C=N

stretching vibrations corresponding to four imine groups of the macrocyclic framework were observed at 1640 cm^{-1} in **1** and 1649 cm^{-1} in **2**, indicating the formation of the macrocyclic complexes [12]. In addition, strong bands at 1578 and 1420 cm^{-1} for **1**, and 1584 and 1436 cm^{-1} for **2** can be ascribed to the asymmetric and symmetric stretching vibration of $-COO^-$ of the complexes [12]. The separation between the two modes is less than 200 cm^{-1}, indicating bidentate coordination of carboxylate [13], which is confirmed by X-ray crystallography. The strong bands at 1095 and 622 cm^{-1} for **1** and 1121 and 620 cm^{-1} for **2** may reasonably be assigned to ClO_4^-. The unresolved bands at 1070 cm^{-1} for **1** and 1121 cm^{-1} for **2** suggest that ClO_4^- is not coordinated to metal in the solid state [14], also in accord with the crystal structures of the complexes.

3.2. *Electrospray mass spectra*

The ES-MS spectra of the complexes were measured in methanol solution (S1). A dominant peak at m/z 270.6 (100%) and another peak at m/z 600.5 (56%) were assigned to $[Zn_2L]^{2+}$ and $[Zn_2L(OAc)]^+$ for **1**, respectively, which can be ascribed to the molecular ionic peak of the complex, and confirm the formation of the macrocyclic complex. Similar to the assignments of peaks in **1**, **2** exhibits molecule-ion peaks of $[Mn_2L(OAc)]^+$ and $[Mn_2L]^{2+}$ at m/z 260.2 (100%) and 579.5 (62%). No other peaks in ES-MS spectra of the complexes are observed except these molecular ion peaks, illustrating that the complexes are very stable in methanol solution [9].

3.3. *Crystal structure of complexes*

The perspective view of $[Zn_2L(OAc](ClO_4)$ (**1**) and $[Mn_2L(OAc)_2]\cdot 4H_2O$ (**2**) are given in figure 1 with the atom numbering scheme. Crystallographic data and details about the data collection are presented in table 1 and selected bond lengths (Å) and angles (°) relevant to the metal(II) coordination spheres of the two complexes are listed in table 2. The shape of the complexes are a little different from that of $[Cu_2L(\mu\text{-}ClO_4)_2]$ [15]; the latter displays a cockleshell shape, while the former presents a compressed shape.

3.3.1. $[Zn_2L(OAc](ClO_4)$. $[Zn_2L(\mu\text{-}OAc](ClO_4)$ has a C_2 axis at the center of Zn(II)–Zn(II) axis, which is perpendicular to the macrocyclic plane. The zinc–zinc separation bridged by two phenolic oxygens is 3.021 Å with Zn–O–Zn angles of 93.4 and 94.5°, respectively. The coordination polyhedra of each Zn(II) can be described approximately as square pyramidal. The basal coordination plane of each Zn(II) is composed of two imine nitrogens and two phenoxides with Zn(II)-donor distances from 2.033 to 2.093 Å. The apical positions are occupied by oxygens from μ_2-OAc^- with Zn–O distances of 1.986 and 1.975 Å, respectively, shorter than that of analogues [16]. The Zn(II)'s depart 0.4626 and 0.5057 Å from the mean N_2O_2 basal plane in one side of the macrocycle.

The macrocyclic units form dimers in opposite arrangement through hydrogen-bond interactions (C–H···O) (figure 2). The dimers are linked by perchlorate through C–H···O (C13–H13···O13, C7–H7···O13, and C22–H22B···O11) hydrogen bonds in the *ab* plane to form a sheet structure (S2). These sheets stack acclivitous in the *c*-axis to form a 3-D network through C–H···O (C5–H5···O14) hydrogen bonds.

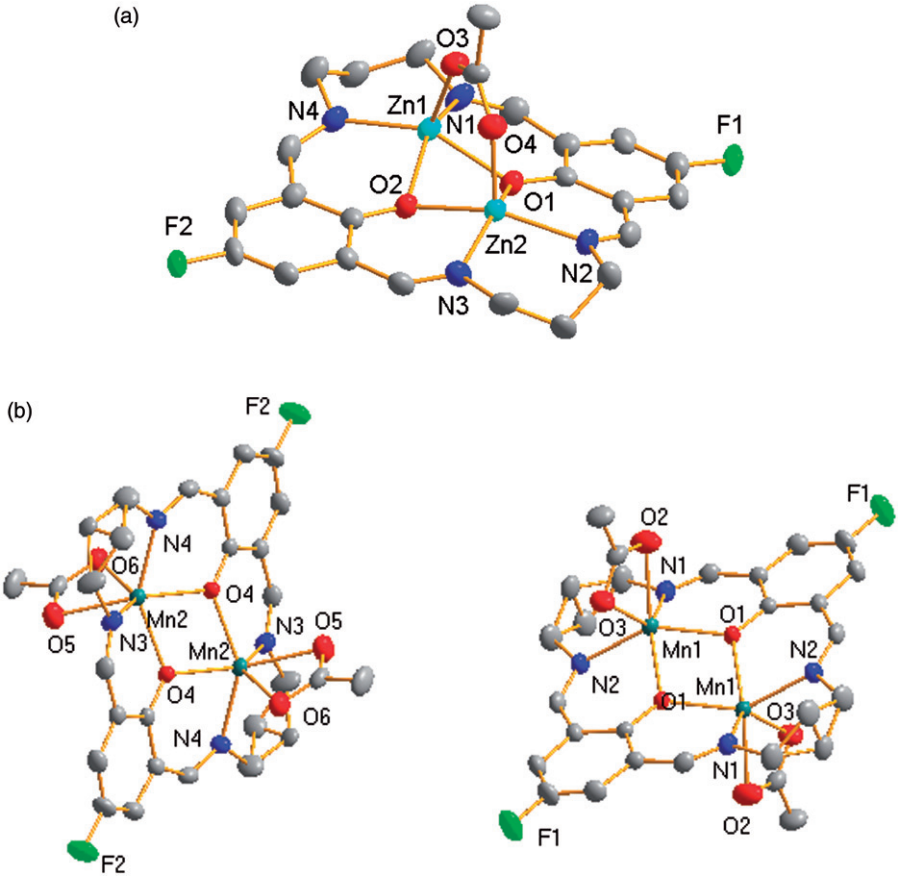

Figure 1. ORTEP view of: (a) $[Zn_2L(OAc)](ClO_4)$; (b) $[Mn_2L(OAc)_2]\cdot 4H_2O$.

The H···O distances range from 2.507 to 2.602 Å, comparable to those reported [17]. The perchlorates play a key role in maintaining the 3-D network of the complex.

3.3.2. $[Mn_2L(OAc)_2]\cdot 4H_2O$. The macrocyclic ligand in **2** is the same as that in **1**. Complex **2** contains two similar macrocyclic units (**A** and **B**), and there is a symmetric center in the middle of the Mn–Mn axis of the units. The units display a flat structure, two manganeses depart from the macrocycle 0.7519 Å in the opposite side, different from **1**. The coordination polyhedra of manganese present a cuneiform structure, and the Mn-donor distances are in the range of 2.206–2.120 Å in macrocyclic planes, while Mn–O (OAc) distances are 2.248 and 2.303 Å. Although the coordination environment is similar between **A** and **B**, the bond lengths and angles are different, with averages of Mn–N and Mn–O distances in unit **A** shorter than in unit **B**. The stacking diagram along the *bc* plane of **2** is shown in figure 3. Macrocyclic units, **A** or **B** defined by Mn1 or Mn2, respectively, are in a line forming 1-D chain structures through the C–H···F hydrogen bonds between two adjacent phenyls with H···F distance 2.468 Å for **A** and 2.440 Å for **B** (figure 3). The chains are parallel to each other with offset arrangement

Table 1. Crystal data and structure refinements for **1** and **2**.

Empirical formula	$C_{24}H_{23}ClF_2N_4O_8Zn_2$ (**1**)	$C_{26}H_{34}F_2Mn_2N_4O_{10}$ (**2**)
Formula weight	699.65	710.45
Mo-Kα radiation (Å^3)	0.71073	0.71073
Crystal system	Monoclinic	Monoclinic
Temperature (K)	291(2)	294(2)
Space group	*P2(1)/c*	*P2(1)/c*
Unit cell dimensions (Å, °)		
a	10.2225(7)	22.3201(8)
b	17.6250(12)	14.3002(12)
c	14.8856(10)	9.9326(6)
α	90	90
β	95.5960(10)	102.0820(10)
γ	90	90
Volume (Å^3), *Z*	2669.2(3), 4	3100.1(3), 4
Calculated density (g cm^{-3})	1.741	1.522
Absorption coefficient, μ (Moka) (nm^{-1})	1.968	0.886
F(000)	1416	1464
Crystal size (mm^3)	0.24 × 0.26 × 0.28	0.20 × 0.10 × 0.10
θ range for data collection (°)	2.0–26.0	1.70–27.00
*N*ref, *N*par	5255, 371	6760, 444
Tot., uniq. data *R*(int)	15,293, 5255, 0.0408	23,032, 6760, 0.0448
Observed data [$I > 2.0\sigma(I)$]	4044	4763
W^{-1}	$1/[S^2(F_o^2) + (0.05P)^2 + 1.99P]$ $P = (F_o^2 + 2F_c^2)/3$	$1/[S^2(F_o^2) + (0.0574P)^2 + 0.4774P]$ $P = (F_o^2 + 2F_c^2)/3$
R, wR_2, *S*	0.0514, 0.1175, 1.08	0.1145, 1.036, 1.035
Max. and av. shift/error	0.00, 0.00	0.001, 0.000
Min. and max. resd. dens. (e Å^{-3})	−0.45, 0.29	−0.341, 0.378

Table 2. Selected bond lengths (Å) and angles (°) for **1** and **2**.

1				**2**			
Bond lengths (Å)		Bond lengths (Å)		Bond lengths (Å)		Bond lengths (Å)	
Zn1–O1	2.082(3)	Zn2–O1	2.034(3)	Mn1–O1	2.1200(19)	Mn2–O4	2.1257(18)
Zn1–O2	2.093(3)	Zn2–O2	2.059(3)	Mn1–O1′	2.1445(18)	Mn2–O4′	2.1368(17)
Zn1–O3	1.985(3)	Zn2–O4	1.975(3)	Mn1–N2	2.200(3)	Mn2–N4	2.205(2)
Zn1–N1	2.060(4)	Zn2–N2	2.051(4)	Mn1–N1	2.206(2)	Mn2–N3	2.201(2)
Zn1–N4	2.049(4)	Zn2–N3	2.064(4)	Mn1–O3	2.248(2)	Mn2–O6	2.269(2)
				Mn1–O2	2.303(2)	Mn2–O5	2.304(2)
Bond angles (°)		Bond angles (°)		Bond angles (°)		Bond angles (°)	
O1–Zn1–O2	74.21(11)	O1–Zn2–O2	75.97(12)	O1–Mn1–O1′	76.08(8)	O4–Mn2–O4′	75.43(8)
O1–Zn1–O3	95.84(13)	O1–Zn2–O4	100.82(12)	O1–Mn1–N2	141.49(9)	O4–Mn2–N3	83.57(8)
O1–Zn1–N1	88.75(13)	O1–Zn2–N2	88.16(14)	O1′–Mn1–N2	83.04(8)	O4′–Mn2–N3	134.40(9)
O1–Zn1–N4	151.61(15)	O1–Zn2–N3	150.46(15)	O1–Mn1–N1	83.67(8)	O4–Mn2–N4	142.02(9)
O2–Zn1–O3	101.78(13)	O2–Zn2–O4	96.84(13)	O1′–Mn1–N1	135.98(9)	O4′–Mn2–N4	83.66(8)
O2–Zn1–N1	147.86(15)	O2–Zn2–N2	153.01(15)	N2–Mn1–N1	89.66(9)	N3–Mn2–N4	89.21(9)
O2–Zn1–N4	88.70(14)	O2–Zn2–N3	87.23(13)	O1–Mn1–O3	123.32(9)	N4–Mn2–O6	90.39(9)
O3–Zn1–N1	107.00(16)	O4–Zn2–N2	107.64(15)	O1′–Mn1–O3	89.98(8)	N4–Mn2–O6	90.40(9)
O3–Zn1–N4	109.96(15)	O4–Zn2–N3	105.22(15)	N2–Mn1–O3	88.14(9)	O4–Mn2–O5	96.55(9)
N1–Zn1–N4	94.60(16)	N2–Zn2–N3	96.93(16)	N2–Mn1–O2	119.42(10)	O6–Mn2–O5	56.18(9)

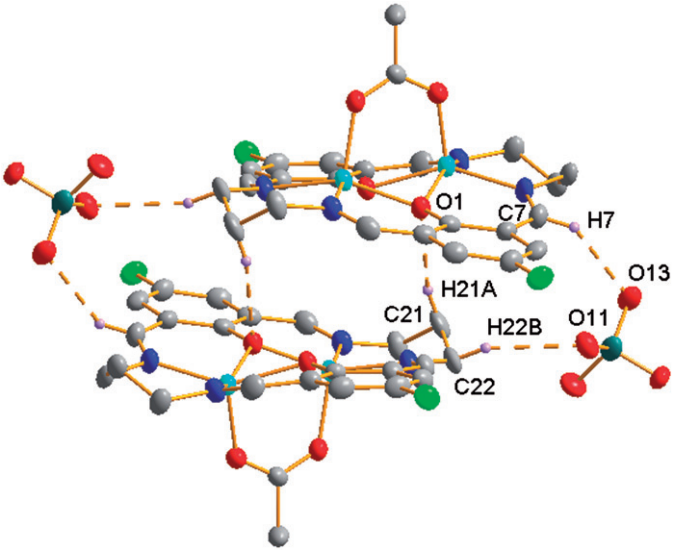

Figure 2. The dimer of **1** formed through hydrogen bonds.

between **A**/**B** units through C–H···O hydrogen bonds with H···O distances 2.615/2.576 Å along the *c*-axis to construct a 2-D sheet structure (Supplementary materials).

The most striking feature is that the crystalline waters form two kinds of 1-D water chains. One of the water chains contains O7/O8 repeating units with O···O distances of 2.808(4) and 2.777(5) Å, respectively. Another contains O9/O10 repeating units with O···O distances of 2.833(5) and 2.793(4) Å, which are slightly larger than relative ones in O7/O8 water chains. These water chains link **A** and **B** alternately along the *a*-axis to form a 3-D structure through strong hydrogen-bond interactions. The interactions are ascribed to those of O–H(water chain)···O(coordinated OAc^-) with the average O···O distances of 2.902 Å (figure 4). The average O···O distances of 2.821 Å between waters is smaller to that of liquid water which shows a value of 2.85 Å [18]. Water–water interactions are stronger than those of water-carboxylate because of shorter O···O distance of the former. Every oxygen in a water chain is a double acceptor and a single donor of H-bonding and has three coordination, less than "formal" four coordination (in a water molecule, two hydrogens are acceptor, and two lone pairs as donors). The hydrogen-bond deficient waters are similar with those at the surface of ice [19]. The two kinds of water chains exhibit similar wave-like chain structure with adjacent O···O···O angles in the water chain containing O9 and O10 of 126.9(1) and 124.5(1)°, while the adjacent O···O···O angles in the other water chain (made from O7 and O8) are 128.8(1) and 127.9(1)°, respectively. Therefore, the water molecules in **2** play a key role in maintaining the 3-D structure of this complex. This is the first example of macrocyclic complexes connected by water chains.

3.4. *Interaction between the complex and plasmid DNA (pBR322)*

DNA cleavage is evaluated by the relaxation modes of supercoiled (SC) circular conformation of *pBR322* DNA, nicked circular (NC), and/or linear conformation.

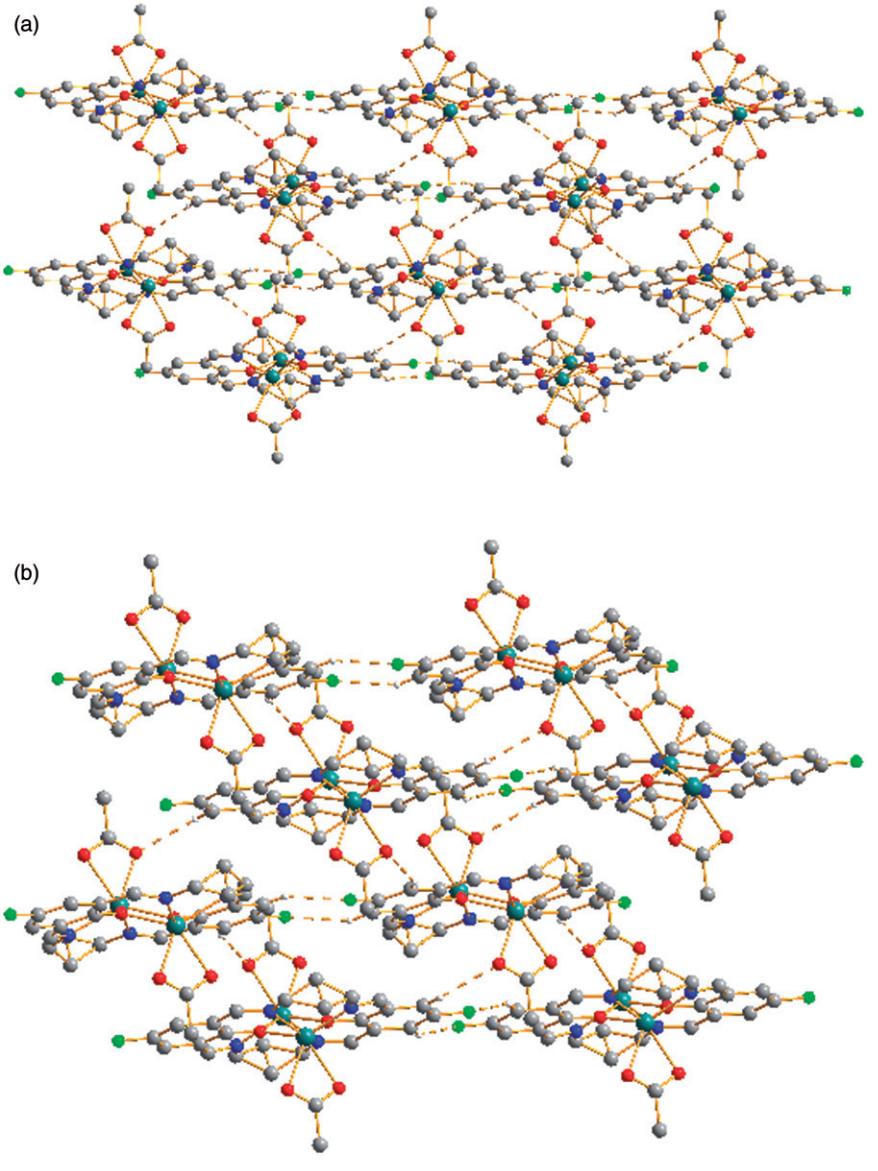

Figure 3. View of the sheet networks along the *bc* plane: (a) for unit **A** and (b) for unit **B**.

When electrophoresis is applied to circular plasmid DNA, a fastest migration will be observed for DNA of closed circular conformation (Form I). If one strand is cleaved, the supercoil will relax to produce a slower-moving nicked conformation (Form II). If both strands are cleaved, a linear conformation (Form III) will be generated that migrates in between [20].

Figure 5 shows the results of gel electophoretic separations of *pBR322* DNA by an increasing amount of the complexes in air. Form I *pBR322* DNA is gradually converted into Form II or Form III counterparts. The DNA cleavage abilities of the complexes

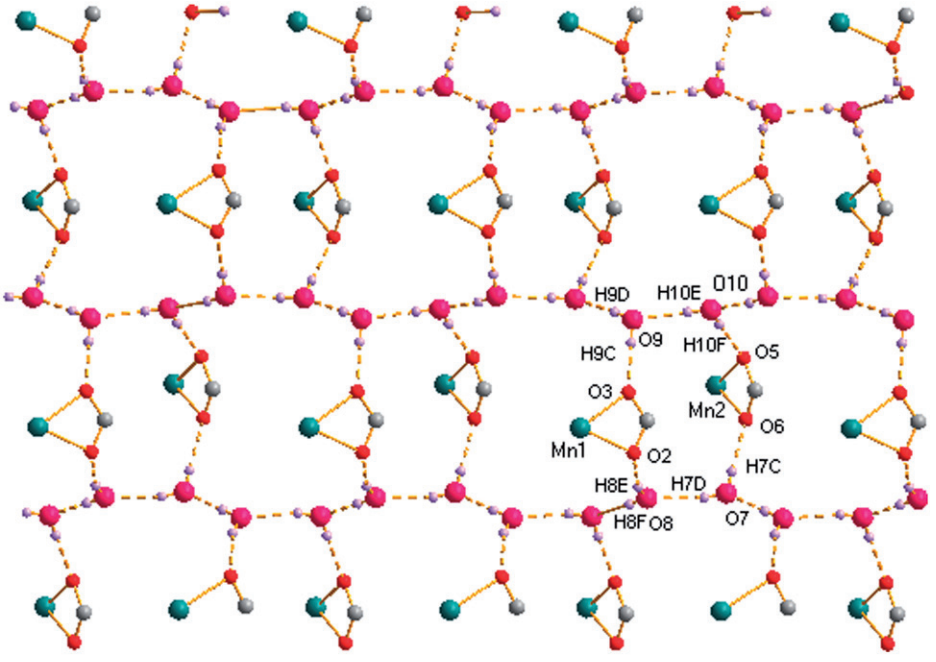

Figure 4. A perspective view of the water chains (O7/O8 and O9/O10) showing how they are connecting with macrocyclic **A** and **B** (represented by Mn1 and Mn2 for clarity).

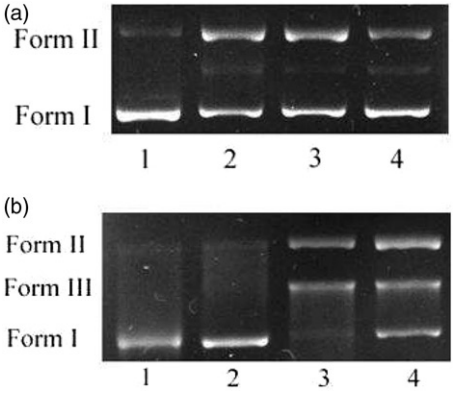

Figure 5. Cleavage of *pBR322* DNA by **1** and **2** at different concentration after 3 h incubation at room temperature. (a) Lane 1: DNA (control); Lanes 2–4: DNA + **1** (400, 200, 100 μmol L^{-1}); (b) Lane 1: DNA (control); Lanes 2–4: DNA + **2** (100, 400, 200 μmol L^{-1}).

were initially studied by monitoring the conversion of circular SC DNA to NC DNA. Complex **1** cleaves *pBR322* plasmid DNA to NC Form II at 100 μmol L^{-1}, while **2** cleaves *pBR322* plasmid DNA to NC Form II and linear Form III, which indicate that the DNA cleavage ability of **2** is much greater than that of **1**. Comparing with other macrocyclic complexes [21] the DNA cleavage activities of the complexes are higher for they cleave SC DNA to NC DNA in the absence of H_2O_2.

Table 3. The diameters of inhibition against *E. coli* and *S. aureus* (mm).

	E. coli		*S. aureus*	
	192 mmol L^{-1}	0.96 mmol L^{-1}	192 mmol L^{-1}	0.96 mmol L^{-1}
Complex **1**	11	10	13	11
Penicillin	14	13	12	11
Complex **2**	11	7	10	7
Penicillin	12	10	14	12

3.5. *Antibacterial activity*

The ligands, solvent (DMSO), and their metal complexes were screened for antibacterial activities. Table 3 shows the antibacterial activities of the prepared compounds, which were evaluated by a well-diffusion method against Gram-positive and Gram-negative bacteria with penicillin as control. Activities against *E. coli* were increased gradually with increasing concentration of the complexes, but lower than that of penicillin, due to the thick cell membrane of *E. coli* against endosmosis of the reagent. The activities against *S. aureus* were also increased with increasing concentration of the complex, and the antibacterial activities were higher than against *E. coli* and comparable to that of penicillin. These results are consistent with previous reports [22].

4. Conclusion

Reactions between ethylenediamine and 2,6-diformyl-4-fluorophenol in the presence of M(II) (M = Zn and Mn) have produced dinuclear complexes of [2 + 2] Schiff base ligands. Although both complexes have the same macrocyclic ligand, the self-assembly behaviors are different due to the difference in metal. Hydrogen-bonding interactions are primary in the 3-D networks of the complexes. 1-D water chains in **2** connect macrocyclic units through strong hydrogen-bond interactions, reported here for the first time. DNA cleavage activity of **2** is higher than that of **1**. Antibacterial activities of **1** are comparable to that of penicillin and those of **2** are slightly less than that of penicillin, indicating that the metal ions play an important role in bioactivities. Complex **2** exhibited higher biological activities than open chain Schiff base dinuclear Zn complexes [23]. We propose that the macrocyclic Schiff-base metal complexes have higher stability than open chain complexes in aqueous solution. Further investigations to identify the relationship between stability and activity are currently underway in our lab.

Acknowledgments

We greatly appreciate the foundation for midlife and youth excellent innovation group of Hubei Province, China (No. T200802), National Nature Science Foundation of China (Nos. 20871097, 20971102 and 21002076) for financial support.

References

[1] For recent reviews: (a) N.E. Borisova, M.D. Reshetova, Y.A. Ustynyuk. *Chem. Rev.*, **107**, 46 (2007); (b) J. Durand, B. Milani. *Coord. Chem. Rev.*, **250**, 542 (2006); (c) I.V. Korendovych, R.J. Staples, W.M. Reiff, E.V. Rybak-Akimova. *Inorg. Chem.*, **43**, 3930 (2004); (d) K. Campbell, R. McDonald, R.R. Tykwinski. *J. Org. Chem.*, **67**, 1133 (2002).

[2] For selected reviews, see: (a) P.J. Chmielewski, L. Latos-Grazynski. *Coord. Chem. Rev.*, **249**, 2510 (2005); (b) F.C. Schroder, J.J. Farmer, A.B. Attygalle, S.R. Smedley, T. Eisner, J. Meinwald. *Science*, **281**, 428 (1998); selected examples: (c) D.K. Chand, H.J. Schneider, A. Bencini, A. Bianchi, C. Giorgi, S. Ciattini, B. Valtancoli. *Chem. Eur. J.*, **6**, 4001 (2000); (d) A. Panda, S.C. Menon, H.B. Singh, C.P. Morley, R. Bachman, T.M. Cocker, R.J. Butcher. *Eur. J. Inorg. Chem.*, 1114 (2005).

[3] (a) N.M. Hosny, Y.E. Sherif, A.E. Rahman. *J. Coord. Chem.*, **61**, 2536 (2008); (b) F. Sparatore, G. Pirisino, M.C. Alamanni, P. Manca-Dimich, M. Satta. *Bull. Chim. Farm.*, **117**, 638 (1978).

[4] Selected examples: (a) Z.L. You, H.L. Zhu. *Z. Anorg. Allg. Chem.*, **632**, 140 (2006); (b) S.P. Xu, L. Shi, P.C. Lv, R.Q. Fang, H.L. Zhu. *J. Coord. Chem.*, **62**, 2048 (2009); (c) J.A. Kiehlbauch, G.E. Hannett, M. Salfinger, W. Archinal, C. Monserrat, C. Carlyn. *J. Clin. Microbiol.*, **38**, 3341 (2000).

[5] Selected examples: (a) S.A. Khan, A.A. Siddiqui, B. Shibeer. *Asian J. Chem.*, **14**, 117 (2002); (b) M. Verma, S.N. Pandeya, K.N. Singh, J.P. Stables. *Acta Pharm.*, **54**, 49 (2004); (c) N. Sari, S. Arslan, E. Logoglu, I. Sakiyan. *G. U. J. Sci.*, **16**, 283 (2003).

[6] Selected examples: (a) P. Prusis, M. Dambrova, V. Andrianov, E. Rozhkov, V. Semenikhina, I. Piskunova, E. Ongwae, T. Lundstedt, I. Kalvinsh, J.E.S. Wikberg. *J. Med. Chem.*, **47**, 3105 (2004); (b) S. Ren, R. Wang, K. Komatsu, P. Bonaz-Krause, Y. Zyrianov, C.E. Mckenna, C. Csipke, Z.A. Tokes, E.J. Lien. *J. Med. Chem.*, **45**, 410 (2002).

[7] Y. He, X.-H. Wang, H. Zhou, Z.-Q. Pan, J.-B. Li, Q.-M. Huang. *Inorg. Chem. Commun.*, **13**, 314 (2010).

[8] L. Chen, J.-L. Bai, H. Zhou, Z.-Q. Pan, Q.-M. Huang, Y. Song. *J. Coord. Chem.*, **61**, 1412 (2008).

[9] (a) S.K. Mandal, L.K. Thompson, M.J. Newlands, E.J. Gabe. *Inorg. Chem.*, **28**, 3707 (1989); (b) R.C. Long, D.N. Hendrickson. *J. Am. Chem. Soc.*, **105**, 1513 (1983).

[10] *SMART* and *SAINT. Area Detector Control and Integration Software*, Siemens Analytical X-Ray Systems, Inc., Madison, Wisconsin, USA (1996).

[11] G.M. Sheldrick. *SHELXTL V5.1 Software Reference Manual*, AXS Bruker, Inc., Madison, Wisconsin, USA (1997).

[12] H. Okawa, S. Kida. *Bull. Chem. Soc. Jpn.*, **45**, 1759 (1972).

[13] (a) G. B. Deacon, R.J. Phillips. *Coord. Chem. Rev.*, **33**, 227 (1980); (b) H. Wada, K.I. Motoda, M. Ohba, H. Sakiyama, N. Matsumoto, H. Okawa. *Bull. Chem. Soc. Jpn.*, **68**, 1105 (1995).

[14] K. Nakamoto. *Infrared and Raman Spectra of Inorganic and Coordination Compounds*, 3rd Edn, Wiley-Interscience, New York (1977).

[15] H. Zhou, Z.-H. Peng, Z.-Q. Pan, D.-C. Li, B. Liu, Z. Zhang, R.A. Chi. *J. Mol. Struct.*, **743**, 59 (2005).

[16] W. Huang, S.-H. Gou, D.-H. Hu, Y. Xu, S. Chantrapromma, Q.-J. Meng. *J. Mol. Struct.*, **561**, 121 (2001).

[17] W. Huang, S.-H. Gou, D.-H. Hu, S. Chantrapromma, H.-K. Fun, Q.-J. Meng. *Inorg. Chem.*, **41**, 864 (2002).

[18] W.F. Kuhs, M.S. Lehman. *J. Phys. Chem.*, **87**, 4312 (1983).

[19] C.J. Gruenloh, J.R. Carney, C.A. Arrington, T.S. Zwier, S.Y. Fredericks, K.D. Jordan. *Science*, **276**, 1678 (1997).

[20] (a) A. Sitlani, E.C. Long, A.M. Pyle, J.K. Barton. *J. Am. Chem. Soc.*, **114**, 2303 (1992); (b) D.S. Sigman. *Acc. Chem. Res.*, **19**, 180 (1986).

[21] (a) W. Peng, P. -Y. Liu, N. Jiang, H.-H. Lin, G.-L. Zhang, Y. Liu, X.-Q. Yu. *Bioorg. Chem.*, **33**, 374 (2005); (b) T. Hirohama, H. Arii, M. Chikira. *J. Inorg. Biochem.*, **98**, 1778 (2004).

[22] M.C. Rodríguez-Argüelles, R. Cao, A.M. García-Deibe, C. Pelizzi, J. SanmartínMatalobos, F. Zani. *Polyhedron*, **28**, 2187 (2009).

[23] See a recent example: N. Raman, A. Sakthivel, R. Jeyamurugan. *J. Coord. Chem.*, **63**, 1080 (2010).